Journal of Engineering Physics and Thermophysics, Vol. 73, No. 4, 2000

NUMERICAL ANALYSIS OF THE INFLUENCE OF THE ANGLE OF ATTACK ON A TURBULENT FLOW ON AN INCOMPRESSIBLE FLUID PAST A PROFILE OF LARGE THICKNESS WITH VORTEX CELLS

P. A. Baranov, S. A. Isaev, Yu. S. Prigorodov, and A. G. Sudakov

UDC 532.517.4

On the basis of a numerical solution, by the finite-volume method, of the Reynolds equations closed by means of a two-parameter dissipative model of turbulence the authors refine the mechanism of reduction of the head resistance and achievement of high quality of profiles of large thickness by intensification of the flow in the vortex cells on the contour with account for the influence of the Reynolds number and the angle of attack.

1. One of the topical trends in present-day aerohydromechanics is associated with the use of systems of flow control using vortex cells intensified by one or another method of momentum generation. An example of design implementation of this concept can be provided by the promising aircraft "EKIP" that has the geometry of a thick wing and uses a power unit for the functioning of a system of suction from vortex cells along the contour of the aircraft [1].

Scientific justification of this method of flow control, which holds much promise, involves comprehensive studies within the framework of numerical modeling of flow past bodies of different geometry with vortex cells. Using a solution of the problem of flow past a circular cylinder with elliptical cells on its contour as an example, the authors show [2] a change in the spectrum of laminar flow past a body with momentum generated along the generatrices of the cells and a decrease in its head resistance. The same method of flow intensification in small-scale vortex cells is used in [3], where laminar flow past a thick profile with vortex cells is considered. The authors demonstrated the possibility of radical rearrangement of the flow pattern associated with passage from a separating mode of flow past the profile to a nonseparating mode. As a consequence, this makes it possible to decrease the head resistance and attain a high aerodynamic quality of the body.

Intensification of the flow in circular vortex cells by rotating a central body and the influence of such cells on laminar steady-state flow past a transverse cylinder at low Reynolds numbers are discussed in [4]. The authors establish a relation between the rotational velocity of the central body and the decrease in the head resistance of the cylinder with a simultaneous decrease in the length of the zone of circulation flow in the wake behind it. In [5], the same method of acting on the flow in the wake is tested in modeling unsteady flow past a cylinder with circular vortex cells. Here, the effect of weakening of the von Kármán vortex street with increase in the rotational velocity of the central bodies accompanied by a decrease in the head resistance of the cylinder is demonstrated. In [6], the laminar unsteady flow past a blunt plate with rounded trailing edges in which circular vortex cells are located is calculated. Rotation of central bodies in the cells can completely change the pattern of flow near the plate by eliminating the von Kármán vortex street that develops behind it. As a result, the flow in the wake acquires a jet character and the head resistance of the layout drops.

The use of suction on the central body as the method of acting on the flow that is traditional in hydromechanics makes it possible to enhance the eddy motion in the cell and to implement small-scale control by exerting an influence on the large-scale character of the flow past an object with cells. In [7], the depend-

Academy of Civil Aviation, St. Petersburg, Russia. Translated from Inzhenerno-Fizicheskii Zhurnal, Vol. 73, No. 4, pp. 719-727, July–August, 2000. Original article submitted September 10, 1999.

ences of the spectrum of turbulent flow near a cylinder with circular cells and its head resistance on the suction velocity on the central body are studied. Here the authors show the existence of different modes of flow around the cylinder that are accompanied by rearrangement of the pattern of flow in the wake and a drop in the head resistance, depending on the location of the cells on the cylinder contour and the intensity of their action on the eddy flow formed within their limits. It should be noted that one of the tasks of this work is to elucidate the mechanism of rearrangement of the structure of the flow around a cylinder on the basis of a thorough analysis of intensification of the eddy flow in a cell. As a whole, the work presented is a continuation of an investigation concerned with evaluation of the efficiency of flow control in numerical modeling of flow past thick profiles with vortex cells [8] with account for a change in the Reynolds number and the angle of attack.

2. The conjugate problem of the influence of trapped small-scale eddy structures on the turbulent flow of an incompressible viscous fluid and the aerodynamic resistance of a circular cylinder and a thick profile with intensification of the flow in vortex cells by means of suction through the central bodies is formulated and solved. The algorithm used is based on the finite-volume method of solution of Reynolds-averaged Navier–Stokes equations that are closed using a high-Reynolds two-parameter dissipative model of turbulence within the framework of the concept of decomposition of the computational region and generation of multiblock oblique-angled grids of the O-type with overlap in singled-out subregions with significantly different scales. This approach seems more universal than that used in [9], where the region of a vortex cell and the region around the body contour had a common boundary.

The initial equations are written in divergent form for increments in the dependent variables: the covariant components of the velocity, pressure, turbulence energy, and its of dissipation rate. The convective flows in the momentum equations are calculated following Leonard's one-dimensional counterflow scheme of quadratic interpolation [10]. For discretization of the convective terms of the equations of transfer of the turbulence characteristics use is made of the UMIST scheme, which is a variant of the TVD scheme [11].

The computational model constructed is based on the concept of splitting by physical processes realized in the SIMPLEC procedure of pressure correction. A characteristic feature of the iterative algorithm of the block type is determination, at the "predictor" step, of preliminary velocity components for "frozen" fields of pressure and turbulent viscosity with a subsequent pressure correction based on a solution of the continuity equation and a correction for the velocity field. At each step the equations for the turbulence characteristics with the "frozen" velocity field are solved by iteration. In the computational procedure, use is made of the method of global iterations in the subregions with subsequent determination of the dependent variables in the zones of overlap of the subregions by the method of conservative interpolation [12]. The multiblock algorithm for calculation of laminar flow in multiply connected regions is described in detail in [5].

Selection of a centered template with coupling of the dependent variables to the center of the computational cell makes it possible to simplify the computational algorithm and decrease the number of the computational operations performed. Here, false oscillations of pressure are suppressed by the Rhee–Chou method. High stability of the computational procedure is ensured by using one-sided counterflow differences for discretization of the convective terms in the implicit side of the equations for the increments in the sought variables, by damping nonphysical oscillations by introduction of artificial diffusion in the implicit part of the equations, and by using pseudo-time stabilizing terms. The efficiency of the computational algorithm is increased in solving the systems of nonlinear algebraic equations by the method of incomplete matrix factorization in Stone's version (SIP). In the calculations, the conventional method of near-wall functions was used [10].

3. In solving the problem of turbulent flow past a transversely oriented cylinder with circular vortex cells, for more exact resolution of structural elements of different scales it seems reasonable to separate the near-wall region with a thickness of about 0.1 of the cylinder diameter (selected as the characteristic dimension), the intermediate circular region encompassing the separation zone in the near wake behind the cylinder, and the peripheral annular zone whose outer boundary is at a rather large distance (of the order of 50–100) from the body. Introduction of several annular zones, which is equivalent to construction of multistage grids, is associated not only with acceleration of the convergence of the solution of the problem due to a decrease in the required number of computational cells but also, what is more important, with setting-up of a local grid for

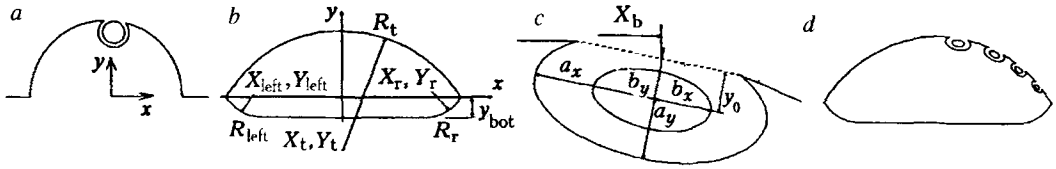

Fig. 1. Scheme of the cylinder with vortex cells (a), contour of the thick profile (b) and the vortex cell (c) with notation, and layout of the cells on the profile (α).

TABLE 1. Results of Numerical and Experimental Studies of the Integrated Characteristics of Turbulent Transverse Flow past a Circular Cylinder

Re	Grid	C_x	C_{xf}	X_s	Ref.
10,000	Multilevel	0.686	0.024	3.96	Present work
10,000	100 × 62	0.743	0.011	5.00	[13]
14,500	–	0.72	–	–	[14]

the characteristics of the mapped structural element of the flow: the boundary layer on the cylinder surface, the return flow in the wake, and the flow past the body at a sufficient distance from it. It should be noted that in the work the results presented are obtained under the assumption of the occurrence of a symmetric mode of flow past the cylinder (Fig. 1a). This allows us to simplify somewhat the solution of the problem by considering the flow in one half-plane. Numerical experiments carried out without this assumption have confirmed the validity of the approach used.

In this investigation, the number of the nodes in the outer zone is chosen equal to 15 × 40, in the intermediate zone 60 × 80, and in the near-wall zone 21 × 80. The step near the wall is 0.0005. Inside the vortex cells (Fig. 1c) the grid is constructed uniformly in the circumferential direction and along the radius (21 nodes are chosen). On the section of the cavity the number of points is prescribed (15 nodes). The total number of points in the circumferential direction is then calculated from the condition of equality of the angular step. The diameter of the vortex cell is taken to be 0.2. The diameter of the central body is 0.144. In all cases the cells are arranged inside the cylinder with a deepening of 15% of the transverse size of the cell ($y_0 = 0.7a_x$). A location of the cell that is displaced downstream from the point of separation in flow past a smooth cylinder and is characterized by the distance $X_b = 0.05$ is considered (Fig. 1c). As follows from an analysis of results of numerical modeling of turbulent flow past a cylinder with various arrangements of vortex cells [7], the chosen version seems the most interesting from the viewpoint of reduction of the head resistance of the cylinder with increase in the suction velocity V_n. The normal component of the suction velocity V_n on the central body of the cell varies in the range of 0–0.05 (in the fractions of the velocity of the oncoming flow). The Reynolds number is prescribed to equal 10^4. An analysis of calculated results for the head resistance C_x, the friction resistance C_{xf}, and the length of the separation zone X_s in the near wake behind a smooth circular cylinder made using available calculated [13] and experimental [14] data at almost the same Re numbers and presented in Table 1 shows the acceptability of the created computational algorithm.

In the absence of suction the vortex cell virtually does not influence the head resistance of the cylinder when the cell is located in the separation zone. In this case, the fluid in the cell does not, in fact, move. Gradually increasing suction of fluid on the central body of the cell causes progressive intensification of the flow in the cavity. However, the curve $C_x(V_n)$, as is seen in Fig. 2c, has a step portion. In the range of V_n of 0.031–0.032, C_x undergoes an almost twofold decrease. The reason for this behavior of the curve $C_x(V_n)$ lies not only in a sharp redistribution of local loads on the cylinder surface but also in transformation of the pattern of flow past it (Fig. 2b). As follows from Fig. 2a, the radical enhancement of the momentum of the turbulent flow in the near-wall zone of the cylinder is caused by the abrupt intensification of the return flow in the cell which, in turn, is associated with its turbulization (Fig. 2b). It should be emphasized that the cylinder resistance is almost halved; moreover, in a significant range of the suction velocity ($V_n > 0.031$) the level of decrease of

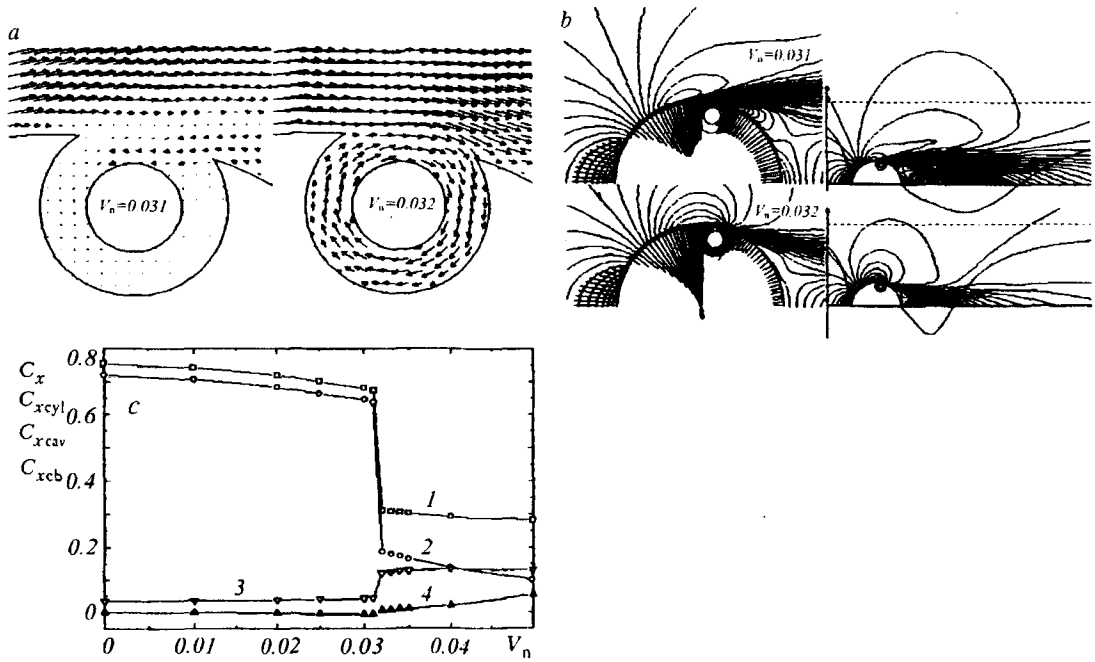

Fig. 2. Stepwise rearrangements of the pattern of turbulent flow in the vortex cell (a) and of the pattern of isolines of the longitudinal velocity around the cylinder, the pressure diagram on its contour, and the velocity distribution in the near wake (b) with the suction velocity changing from 0.031 to 0.032 and a comparison of the dependences of the head resistance of the cylinder and its components on V_n (c) [1-4) C_x, from the top down].

the cylinder resistance is almost constant (Fig. 2c). An analysis of the influence of the suction velocity on the components of the head resistance of the cylinder confirms that the step behavior of C_x is caused, first of all, by the abrupt decrease in the magnitude of its component C_{xcyl} associated with local loads on the cylinder contour, although the component of the head resistance that is determined mainly by the distribution of the static pressure over the walls of the vortex cells also changes abruptly (by a factor of six). It is of interest that the tendencies of change in C_{xcyl} and C_{xcav} turn out to be opposite as V_n increases; starting approximately with V_n = 0.04 the resistance of the vortex cells proper exceeds the resistance of the contour part of the cylinder. Moreover, the l loads on the central bodies also make an increasing contribution to the total head resistance of the arrangement and reach almost 20% at V_n = 0.05. Thus, thorough consideration of the phase of stepwise change in the head resistance of the cylinder with vortex cells indicates that this aerodynamic effect, which is associated with rearrangement of the pattern of flow past the body, is due to a distinctive initiation of turbulent flow in the vortex cell once the suction velocity has reached its threshold value on the central body.

4. The present investigation is also concerned with a thick profile whose top part is a circular arc of radius R_t with center at the point X_t, Y_t, while the bottom part is formed by segments of arcs of right and left circles of small radius (with coordinates of the centers X_r, Y_r, and X_{left}, Y_{left} and radii R_r and R_{left}, respectively) and a plane ($y = y_{bot}$). The contour of the profile and the notation are shown in Fig. 1b; the values of the characteristic dimensions are given in Table 2. In solving this problem we chose the chord of the thick profile as the linear scale.

A series of four elliptic vortex cells with central bodies of the same geometry is incorporated into the profile under consideration. The cell topology is shown in Fig. 1c, while the linear dimensions of the cells and their location relative to the center of the profile (Fig. 1d) are presented in Table 3. The computational complex developed provides for the possibility of prescribing, on the walls of the vortex cells and the central bod-

TABLE 2. Layout of the Thick Profile

X_t	Y_t	R_t	X_r	Y_r	R_r	X_{left}	Y_{left}	R_{left}	y_{bot}
0.0	–0.228	0.577	0.348	0.088	0.175	–0.348	0.088	0.175	–0.086

TABLE 3. Parameters of the Vortex Cells on the Profile and the Two Versions of Suction in the Central Bodies of the Cells

Cell No.	Geometric parameters of the cells						Versions V_n	
	X_{body}	y_0/a_x	a_x	a_y/a_x	b_x/a_x	b_y/b_x	1	2
1	0.0876	–0.7	0.0584	0.5	0.5	0.5	0.05	0.05
2	0.2555	–0.7	0.0487	0.5	0.5	0.5	0.05	0.05
3	0.3649	–0.7	0.0389	0.5	0.5	0.5	0.05	0.075
4	0.4452	–0.7	0.0292	0.5	0.5	0.5	0.05	0.10

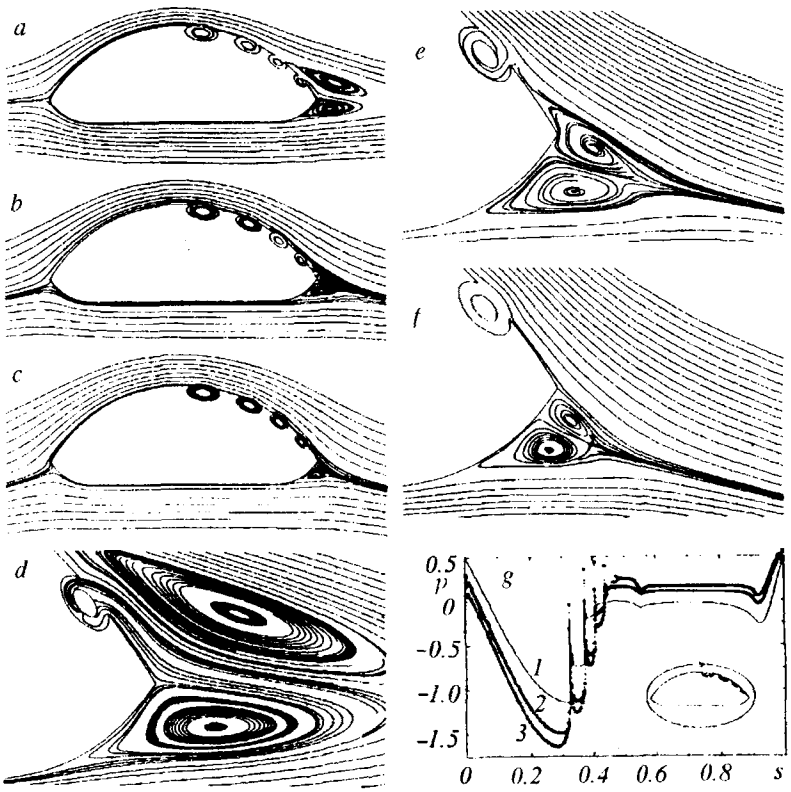

Fig. 3. Comparison of patterns of turbulent flow, for zero angle of attack, past the profile with vortex cells (a, b, c) and its tail part (d, e, f) and of pressure distributions along the profile (g), respectively, for three Reynolds numbers: 1) Re = 10^4; 2) 10^5; 3) 10^6 [1) a, d; 2) b, e; 3) c, f].

ies, velocity components that correspond to injection-suction conditions. The velocity of the oncoming flow is taken to be the scale of the dimensionless representation.

This investigation is restricted to a comparative analysis of two versions with different values of the velocity of suction V_n through the surfaces of the central bodies (see Table 3). The considered model of intensification of the eddy flow in a cell reflects, to some extent, the process of air intake through a porous insert accomplished by its injection using a power unit. As a result of this action, in the cells momentum is brough into the external flow through cuts in the thick profile, which substantially changes the pattern of flow past the profile.

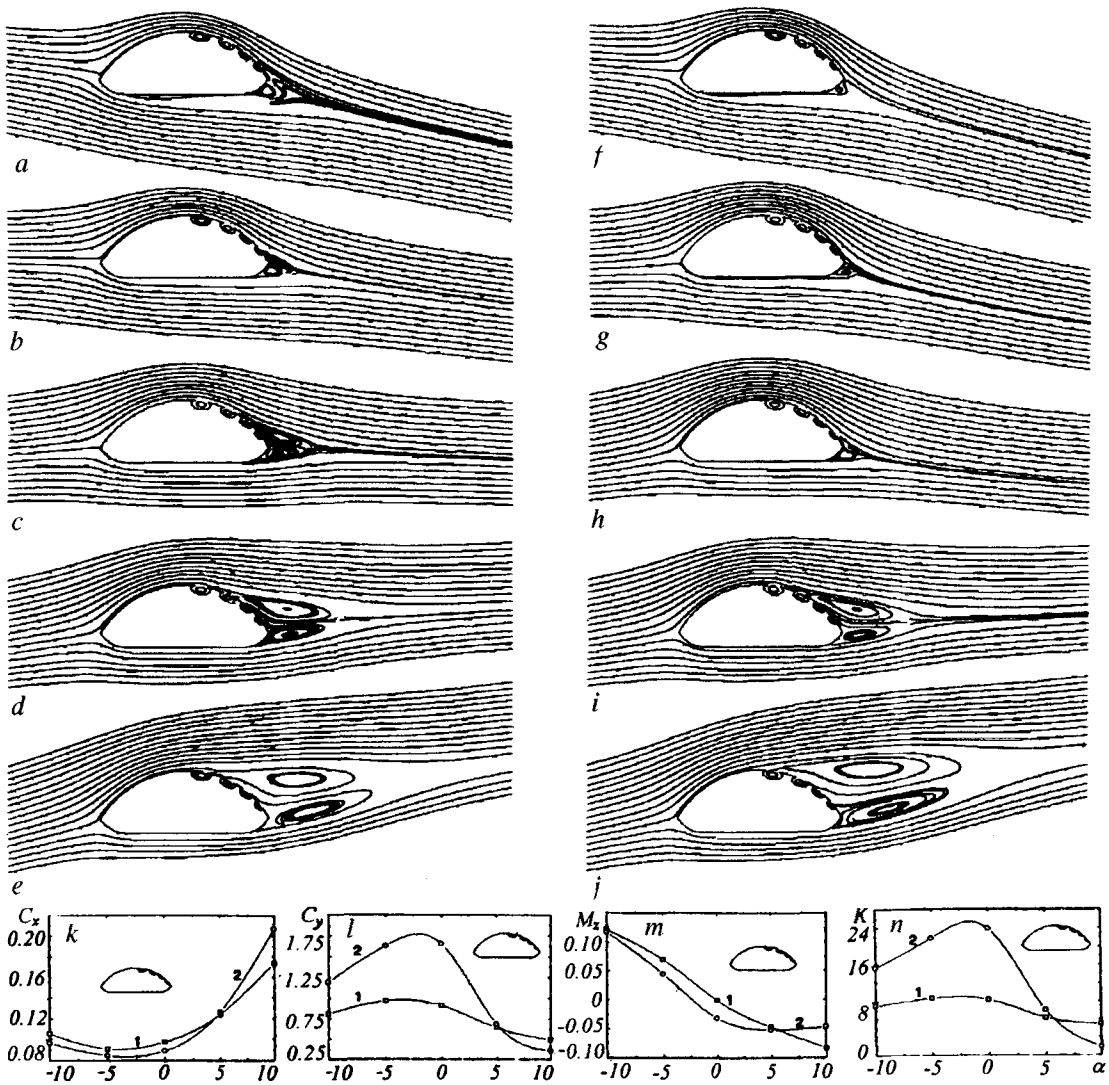

Fig. 4. Comparison of patterns of turbulent flow past the profile with vortex cells for different angles of attack and of dependences of the aerodynamic coefficients of the profile C_x(k), C_y(l), M_z(m), K(n) on the angle of attack for the two versions of suction through the central bodies of the cells: 1) a, b, c, d, e; 2) f, g, h, i, j. The following patterns correspond to the angles of attack: $\alpha = -10^\circ$ (a, f); -5° (b, g); 0° (c, h); 5° (d, i); 10° (e, j).

We construct a nonorthogonal algebraic grid of O-type around the profile. Its first stage adjacent to the contour contains 21 × 200 cells that are arranged with bunching toward the wall in a belt of thickness 0.1. The near-wall step is chosen equal to 0.0005. The second stage consisting of 80 × 120 cells spans the space around the profile to a distance of 80 chords. The vortex cells are subdivided by the O-type grid, in whose radial direction 21 cells are arranged uniformly. The grid is also set uniform in the circumferential direction with 21 cells located in the region of the cut of the profile.

Figures 3, 4 and Table 4 present some of the calculated results obtained for spectra of the flow past the thick profile and distributions of the local and integrated loads on it for different intensities of suction through the central bodies of the vortex cells and variation of the angle of attack from -10° to 10° and the Reynolds number in the range of 10^4–10^6.

TABLE 4. Influence of the Reynolds Number on the Aerodynamic Characteristics of the Thick Profile with Vortex Cells for Velocities of Suction through the Central Bodies Equal to 0.05

Re	C_x	C_{xp}	C_{xf}	C_y	M_z	K
10^4	0.0982	0.0637	0.0345	1.0123	–0.0010	10.308
10^5	0.0674	0.0447	0.0227	1.9924	–0.0314	29.560
10^6	0.0607	0.0549	0.0058	2.4356	–0.0345	40.125

As is shown in [8], at zero angle of attack and Re = 10^4 setting of the suction velocity on the central bodies of the vortex cells equal to 5% of the velocity of the oncoming flow leads to formation of virtually nonseparating flow past the thick profile (Fig. 3a). It should be noted that for the Reynolds number under consideration a small and low-intensity separation region is retained behind the profile, and the last cell also turns out to be passive (Fig. 3d).

As the Reynolds number increases, the circulation flow in the last cells is enhanced, thus promoting the occurrence of completely nonseparating flow past the top part of the profile (Fig. 3b, c). The small separation zone in the tail part is associated with the roundness of the profile at this place and virtually does not cause noticeable deterioration of the aerodynamic characteristics. The high quality of the thick profile (of about 30–40) at high Reynolds numbers is attributed not only to the strong rarefaction on the top surface but also to the decrease in the pressure at the bottom part of the profile caused by the change in the angle at which the flow approaches the profile (Fig. 3g). From Table 4 it follows that the improvement in the aerodynamic quality of the profile with increase in Re is associated with both an increase in the lift coefficient and a decrease in the head-resistance force.

Similarly to [8], in this work consideration is given to enhancement of suction in the rear vortex cells to provide efficiency of all the cells on the contour and formation of a completely nonseparating flow past the top part of the profile for $\alpha = 0^\circ$ and Re = 10^4. The two variants presented in Table 3 are analyzed for various angles of attack and a fixed Reynolds number.

As is seen from Fig. 4, in going from zero to negative (not exceeding 10°) angles of attack the mode of nonseparating flow past the thick profile is preserved; moreover, in the vicinity of the sharp trailing edge the flow becomes smooth due to initiation of the last vortex cell. On the other hand, in going to positive (also not exceeding 10°) angles of attack the flow pattern undergoes rearrangement and forms a developed eddy structure in the near wake nehind the profile. Here, the enhancement of the suction in the vortex cells (version 2) does not exert a marked influence on the character of the separating flow past the profile. At the same time in the case of nonseparating flow past the profile this influence, which is not so pronounced in the vicinity of the profile, substantially modifies the flow in the wake and greatly influences the overall aerodynamic characteristics of the body.

An analysis of the behavior of the aerodynamic coefficients of the profile with variation of α reveals, first of all, the presence of optimum angles of attack α_{opt} differing from zero, at which extreme values of C_x, C_y, K are attained. Whereas for the two considered versions of the suction velocities in the vortex cells the curves $C_x(\alpha)$ and $M_z(\alpha)$ are similar as a whole, $C_y(\alpha)$ and $K(\alpha)$ differ rather significantly. It should be noted that the maximum values of the lift coefficient and the aerodynamic quality (of the order of 25) show more than a twofold increase for the second version of the profile. One more interesting feature that is characteristic of a thick profile with vortex cells is a negative moment of pitch that progresses with increase in α, thus promoting pulling of the aircraft into a dive.

As a whole, the method of efficient control of flow past thick profiles with vortex cells with air suction through central bodies is acceptable in wide ranges of the angle of attack and the Reynolds number. By intensifying the large-scale vortex structures trapped in the cells additional momentum is imparted to the surface layers of the profile, with the air suction working on vortex swirling.

The authors express their thanks to Academician G. G. Chernyi and Academician A. I. Leont'ev for useful discussions of the problem.

This work was carried out with financial support from the Russian Fund for Fundamental Research, projects 99-01-01115 and 99-01-00772.

NOTATION

x, y, longitudinal and transverse Cartesian coordinates; s, relative distance along the body contour measured counterclockwise; X, Y, R, coordinates of the centers of the circles whose arcs are generatrices of the contour of the profile; X_{body}, coordinate of the center of the cut of the profile at the site of location of the vortex cell; y_0, distance from the center of the cell to the plane of the cut of the profile (submergence of the cell in the contour of the profile); a_x, a_y, semimajor and semiminor axes of the elliptic contour of the vortex cell; b_x, b_y, semimajor and semiminor axes of the elliptic contour of the central body of the vortex cell; p, excess pressure referred to the doubled velocity head; C_x, C_{xp}, C_{xf}, coefficients of head and profile resistances and friction force; C_{xcyl}, C_{xcav}, C_{xcb}, components of the head resistance associated with loads on the cylinder contour, the vortex-cell wall, and its central body, respectively; C_y, lift coefficient; M_z, coefficient of pitching moment; K, aerodynamic quality; V_n, suction velocity on the central body; α, angle of attack. Subscripts: t, r, left, top, right, and left arcs of the contour; bot, bottom part of the contour.

REFERENCES

1. A. I. Savitsky, L. N. Shchukin, V. G. Karelin, et al., *US Patent* 5417391 (1995).
2. P. A. Baranov, S. A. Isaev, Yu. S. Prigorodov, and A. G. Sudakov, *Pis'ma Zh. Tekh. Fiz.*, **24**, No. 8, 33-41 (1998).
3. P. A. Baranov, S. A. Isaev, Yu. S. Prigorodov, and A. G. Sudakov, *Izv. Vyssh. Uchebn. Zaved. Aviats. Tekh.*, No. 3, 30-35 (1999).
4. S. A. Isaev, P. A. Baranov, A. E. Usachev, and D. P. Frolov, in: *Proc. 8th Int. Symp. on Flow Visualization*, Sorrento, Sept. 1-4 (1998), pp. 217.1-217.8
5. P. A. Baranov, V. Z. Zhdanov, and A. G. Sudakov, *Numerical Analysis of Unsteady Flow past a Cylinder with Introduction of Induced Vorticity into the Near Wake*, Preprint No. 5 of the Academic Scientific Complex "A. V. Luikov Heat and Mass Transfer Institute," National Academy of Sciences of Belarus [in Russian], Minsk (1998).
6. V. L. Zhdanov, A. G. Sudakov, A. E. Usachev, and D. P. Frolov, *Numerical Analysis of the Unsteady Wake behind a Plate with Rotating Aftercylinders,* Preprint No. 5 of the Academic Scientific Complex "A. V. Luikov Heat and Mass Transfer Institute," National Academy of Sciences of Belarus [in Russian], Minsk (1999).
7. P. A. Baranov, S. A. Isaev, Yu. S. Prigorodov, and A. G. Sudakov, *Pis'ma Zh. Tekh. Fiz.*, **24**, No. 17, 16-23 (1998).
8. P. A. Baranov, S. A. Isaev, Yu. S. Prigorodov, and A. G. Sudakov, *Inzh.-Fiz. Zh.*, **72**, No. 3, 572-575 (1999).
9. P. A. Baranov, S. A. Isaev, Yu. S. Prigorodov, and A. G. Sudakov, *Inzh.-Fiz. Zh.*, **71**, No. 6, 1116-1120 (1998).
10. I. A. Belov, S. A. Isaev, and V. A. Korobkov, *Problems and Methods of Calculation of Separated Flows of Incompressible Fluids* [in Russian], Leningrad (1989).
11. F. S. Lien, W. L. Chen, and M. A. Leschziner, *Int. J. Numer. Meth. in Fluids*, **23**, 567-588 (1996).
12. A. A. Aganin and V. B. Kuznetsov, in: *"Dynamics of the Envelopes in a Flow," Proc. of the Workshop* [in Russian], Issue 18, Kazan (1985), pp. 144-160.
13. I. A. Belov and N. A. Kudryavtsev, *Heat Transfer and Resistance of Stacks of Pipes* [in Russian], Leningrad (1987).
14. A. Roshko, *NACA Tech. Note*, No. 3169 (1954).